

## Distributed Radar Information Fusion for Gait Recognition and Fall Detection

Li, Haobo; Le Kernec, Julien; Mehul, Ajay ; Fioranelli, Francesco

**DOI**

[10.1109/RadarConf2043947.2020.9266319](https://doi.org/10.1109/RadarConf2043947.2020.9266319)

**Publication date**

2020

**Document Version**

Final published version

**Published in**

2020 IEEE Radar Conference, RadarConf 2020

**Citation (APA)**

Li, H., Le Kernec, J., Mehul, A., & Fioranelli, F. (2020). Distributed Radar Information Fusion for Gait Recognition and Fall Detection. In *2020 IEEE Radar Conference, RadarConf 2020* (pp. 1-6). Article 9266319 (IEEE National Radar Conference - Proceedings; Vol. 2020-September). IEEE.  
<https://doi.org/10.1109/RadarConf2043947.2020.9266319>

**Important note**

To cite this publication, please use the final published version (if applicable).  
Please check the document version above.

**Copyright**

Other than for strictly personal use, it is not permitted to download, forward or distribute the text or part of it, without the consent of the author(s) and/or copyright holder(s), unless the work is under an open content license such as Creative Commons.

**Takedown policy**

Please contact us and provide details if you believe this document breaches copyrights.  
We will remove access to the work immediately and investigate your claim.

***Green Open Access added to TU Delft Institutional Repository***

***'You share, we take care!' - Taverne project***

**<https://www.openaccess.nl/en/you-share-we-take-care>**

Otherwise as indicated in the copyright section: the publisher is the copyright holder of this work and the author uses the Dutch legislation to make this work public.

# Distributed Radar Information Fusion for Gait Recognition and Fall Detection

Haobo Li, Julien Le Kernec  
James Watt School of Engineering  
University of Glasgow  
Glasgow, United Kingdom  
h.li.4@research.gla.ac.uk;  
Julien.Lekernec@glasgow.ac.uk

Ajay Mehul,  
Sevgi Zubeyde Gurbuz  
Department of Electrical and Computer  
Engineering  
University of Alabama  
Tuscaloosa, USA  
ajaymehul2013@gmail.com;  
sevgigurbuz@gmail.com

Francesco Fioranelli  
Microwave Sensing Signals & Systems  
(MS3), Department of Microelectronics  
Delft University of Technology  
Delft, The Netherlands  
F.Fioranelli@tudelft.nl

**Abstract**—This paper discusses a fusion framework with data from multiple, distributed radar sensors based on conventional classifiers, and transfer learning with pre-trained deep networks. The application considered is the classification of gait styles and the detection of critical accidents such as falls. The data were collected from a network comprised of one Ancortek frequency modulated continuous wave radar and three ultra wide-band Xethru radars. The radar systems within the network were placed in three different locations, notably, in front of participants, on the ceiling, and on the right-hand side of the monitored area. The proposed information fusion framework compares feature level fusion, soft fusion with the classifier confidence level, and hard fusion with Naïve Bayes combiner (NBC). Regarding the classifier, linear SVM, Random-Forest Bagging Trees, and five pre-trained neural networks are introduced to the fusion algorithm, where the VGG-16 network yields the best performance (about 84%) with the help of NBC. Compared to the best cases with conventional classifiers, it is reported that 20% and 16% subsequent improvement are achieved for individual usage of single radar and fusion.

**Keywords**—radar network, information fusion, multiple radar sensing, machine learning, transfer learning

## I. INTRODUCTION

The growing aging population [1] in western countries and Asia creates significant challenges in providing comprehensive medical care to elderly people with underlying health conditions and timely support after a critical accident such as fall and stroke. Falls usually cause physical injuries [2], [3] including head trauma, face, and hip fracture. These lead to further psychological problems [2], [4] like loss of interest in exercise and fear of being alone. In the UK, the National Health Service spent more than 4 million pounds per day to hospitalize the elderly over 65 years that experienced an accidental fall [5], and this budget has to increase year-by-year because fall may trigger other chronic issues. Researchers found that the life expectancy [6] of the elderly is highly related to the waiting time to receive assistance after the accidents. Thus, a fast-responding and reliable fall detection system [7] can notify the emergency department in the hospital or personal caregivers to provide prompt help. Furthermore, increased fall risk and health anomalies in older people have been correlated with changes in their gait patterns [6], [8]–[10], and related metrics such as asymmetries, slower and less continuous gait, and shorter stride.

Radar is irreplaceable as a contactless sensing technology in many outdoor applications in defense and security. Recently radar has also gained much interest in the context of indoor ambient assisted living [11]. Compared to wearable devices [12], [13] and image/video sensors [14], radar can avoid issues of users' compliance and acceptance due to privacy (no plain images of people or private environments are collected) and/or comfort (no devices to wear, carry, recharge). Radar can also work in through-wall conditions in indoor environments [15] and can provide an estimate of the physical distance and velocity (measured by the Doppler effect) over time for the monitored subjects [16].

Given the many different types and styles of gaits people can show while they move, developing radar-based capable classification algorithms is a fundamental challenge. Convolutional Neural Networks (CNN) [17] have shown higher potential than conventional classifiers in terms of their classification accuracy. However, those improvements come at a price. They require large amounts of data and computational load as more layers are added, which in turn increase the number of hyper-parameters to tune [18]. Transfer learning frameworks have been applied to address this issue. Pre-trained networks such as AlexNet (2012)[19], GoogLeNet (2014)[19], VGG-16 (2016) [20] and ResNet family (2018) have been utilized in classifying radar spectrograms and cepstrum maps, exploiting the deep classification capabilities they gained from prior pre-training with hundred thousands of optical images. This transfer learning method suits a small experimental radar dataset that would not be enough for feeding and training from scratch a traditional CNN.

In this paper, we investigate the transfer learning framework combined with information fusion from a network consisting of four independent but synchronized radar sensors. The sensors are not clocked by the same reference, but they operate simultaneously and collect data at the same time allowing comparisons as a function of spatial position (three identical UWB X-band radar located at three different positions with respect to the subject), as well as of radar frequency (2 co-located radar sensors operating at different frequencies, namely X-band and K-band). In this initial study, we focus on comparing different pre-trained deep network architectures with information fusion schemes, including feature fusion [11], soft decision fusion, and hard decision fusion [21]. The dataset used for the analysis contains 12 different types of gait performed by 14 volunteers, with more details given in the following sections. The initial performance results show that transfer learning can outperform conventional classifiers using manual features and that fusing

The authors acknowledge the support of the UK EPSRC (grant INSHEP EP/R041679/1), University of Glasgow mobility scholarship for PGR students, and GBCET Great Britain China Educational Trust) support for part of the last year of Ph.D studies of Haobo Li.

information from the distributed radar sensors in the network is also beneficial.

The remainder of this paper is organized as follows. Section II introduces the radar network setup and describes the gait data collection. Section III discusses the data processing and classification using a conventional classifier and pre-trained nets. Section IV presents the results of different information fusion approaches. Finally, section V concludes the paper and outlines possible directions for future work.

## II. EXPERIMENTAL SETUP

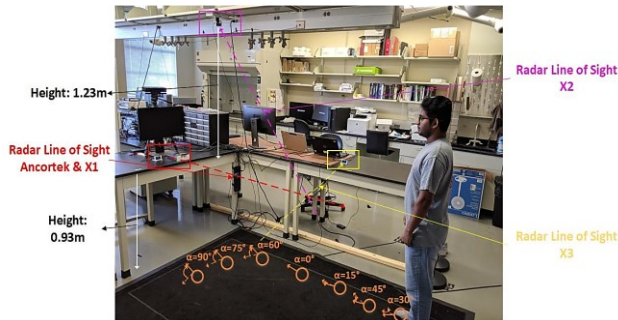


Fig. 1. Experimental setup and walking trajectory. Red line: Ancortek and Xethru in front of the participants; purple line: Xethru on the ceiling; yellow line: Xethru on the right hand side; orange dots on the ground: elliptical trajectory performed by the subjects.

TABLE I. LIST OF THE DIFFERENT GAITS TO BE CLASSIFIED

G1	Walking normally
G2	Walking quickly
G3	Walking slowly
G4	Dragging one foot
G5	Limping with an orthopedic cast
G6	Small steps
G7	Walking with a cane
G8	Walking with a walker
G9	Military walking
G10	Bunny jump
G11	Walking and direct fall
G12	Walking and controlled fall

The dataset was collected in the Computational Intelligence for Radar (CI4R) Lab at the University of Alabama; it contains 11 male and three female participants aged from 19 to 44. Table I lists twelve different gaits, including walking with different speed, dragging one foot while walking, moving with small steps, walking with aids, jumping back and forth, as well as some joint gaits (gaits followed by a fall event). In the experiment, the participants are asked to perform 20 s elliptical loops in the different gait styles (with the lab setup and the trajectory shown in Fig. 1), whereas in ‘G11’ and ‘G12’, two kinds of falling are following a short period of walking (12s approximately) to attempt to simulate the sudden loss of consciousness and progressive exhaustion and fall of elderly people, respectively.

One Ancortek FMCW radar operating at 25 GHz and three Novelda Xethru UWB Doppler radars at 7.5 GHz are utilized to measure the gait patterns, simultaneously with three different spatial perspectives as in Fig. 1. The Ancortek radar and one of the Xethru radars (X1) are set on the table in front of the participants (red box in Fig. 1); the second Xethru (X2) is fixed on the ceiling with an elevation angle of about 45° to the center of the experimental zone (purple box in Fig. 1); the last Xethru (X3) is placed at the right-hand side of the participant (yellow box in Fig. 1). The FMCW radar transmits

a chirp signal with 2 GHz bandwidth and 1 kHz PRF (Pulse Repetition Frequency), whereas the Xethru pulse-Doppler radar has 1.5 GHz bandwidth with 500 kHz PRF.

The radar network is constructed by connecting all the individual radar to a laptop via USB cables. It is synchronized by adding a delay function as the two types of radar have different waking up times to compensate. This allows recording simultaneous data from all four radars, although the radars are not coherently synchronized by the same clock. Furthermore, data from the pressure mattress on the floor in Fig. 1 is also collected and can be used as ground truth for the location of the subject and to examine the sequence of the steps in different gaits.

The dataset is saved in a MATLAB cell array, whose dimension is  $m*n*q$ , where  $m$  is the number of participants,  $n$  is the gait class and  $q$  is the number of the 20 s long repetitions of each gait; in our case,  $q$  equals to 3, hence, the total number of observation is 504 ( $14*12*3$ ).

## III. DATA PROCESSING AND ANALYSIS

### A. Conventional Classifier

The radar data can be mapped into three different domains, notably, Range-Time, Range-Doppler, and Doppler-Time, also known as a radar cube when combined [16]. The Range-Time matrix is obtained by applying a 1<sup>st</sup> Fast Fourier Transform (FFT) on the raw amplitude and phase of the FMCW radar data, whereas the Range-Doppler maps are generated by using a 2<sup>nd</sup> FFT along the time axis of the Range-Time matrix for each range bin. The Doppler-Time domain also referred as a spectrogram, is generated by adding the range bins together for each time bin and then using a Short-Time Fourier Transform (STFT) successively to visualize the micro-Doppler signature, which is significant in characterizing periodic motions such as swinging of human legs and arms. Fig. 2 shows the radar spectrograms of different gaits, where the positive Doppler shift represents the stride towards the radar and vice versa. In this paper, we focus on the spectrogram analysis; the window function used in the STFT is a Hamming window with 0.2s length and 95% overlapping.

Some statistical features are extracted to replace the whole spectrogram as the input of the classifier. The radar features inspired from [22], [23] are used in this paper and listed in Table II. They can be divided into physical features and transform-based features, where the physical features include upper envelope, lower envelope (shown in Fig. 2 with red and white lines), centroid and bandwidth of the Doppler spectrogram. Differently from those, transform-based features perform a mathematic transformation such as SVD (Singular Value Decomposition), DCT (Discrete Cosine Transform) and LPC (Linear Predictive Coding) on the spectrogram data to find more information on a specific dimension. Similar features are also generated from Cadence Velocity Diagram (CVD) and radar cepstrum.

Two robust conventional classifiers, notably, linear SVM and Random-Forest (RF) bagging with 200 trees are selected to train the prediction model and evaluate the classification performance. In this paper, a ‘Leaving one participant out’ (L1O) cross-validation method is used to partition the dataset into training and test part, where data from one participant is chosen to evaluate the classification performance, and the rest of the data is used to train the classifier. Every subject in the

dataset is, in turn, the ‘test participant’, and the results are averaged from the 14 iterations. Compared to the conventional ‘k-fold’ or simpler ‘holdout,’ L1O successfully simulates the more realistic scenario that the classifier cannot access all subjects’ data prior to the actual usage, i.e., the classifier needs to deal well with unknown new subjects.

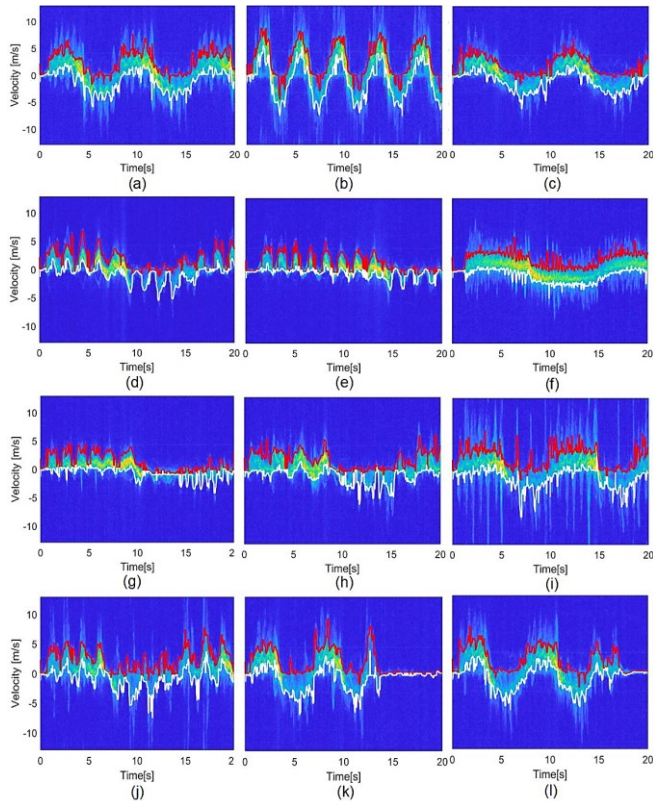


Fig. 2. Ancortek radar spectrograms. The spectrogram from (a) to (l) correspond to the gait from ‘G1’ to ‘G12’ in Table I. Red line: upper envelope, white line: lower envelope.

TABLE II. LIST OF THE RADAR MANUAL FEATURES

Physical features	No. of features
Mean, standard deviation, skewness, and kurtosis of the centroid of the Doppler spectrogram	4
Mean, standard deviation, skewness, and kurtosis of the bandwidth of the Doppler spectrogram	4
Two-dimensional mean, standard deviation, skewness and kurtosis of the whole segment of the spectrogram	4
Mean, maximum and minimum of the upper envelope	3
Mean, maximum and minimum of the lower envelope	3
Difference between the mean of the upper and lower envelope	1
Transform-based features	No. of features
Mean and standard deviation of the first left and right eigenvector of the SVD decomposition of the spectrogram	4
Sum of pixels of the entire left and right matrices	2
Mean of the diagonal of the left and right matrices	2
Discrete DCT of the spectrogram	10
First 10 coefficients of the LPC of the spectrogram	10
Step repetition frequency	1
Step repetition frequency band peak	2
Intensity of the main peak in CVD	1
Maximum of the main peak	1
Energy of the main peak	1
Most significant Doppler frequency in CVD	1
Maximum, minimum and mean of the cepstrum	3
<b>Total number of features</b>	<b>57</b>

The L1O classification results of using radar individually are summarized in Table III, where the Xethru radar in front of the participant outperforms the other radars with SVM, and the Xethru radar on the ceiling yields the best performance with RF Bagging Trees. There is not much difference in Ancortek and X1 using these two classifiers, whereas X2 and X3 share a 5% improvement. Fig. 3 shows in a confusion matrix the misclassification rates between each class, where the rows are output classes, and the columns represent target classes. The diagonal elements are the gaits that are correctly classified, whereas the non-diagonal elements denote the misclassified gaits. The sum of the elements in each column is equal to 100%. This confusion matrix reports high misclassification in ‘G1’, ‘G3’, ‘G5’, and ‘G7’, especially between ‘G1’ and ‘G3’. The walking speed for different people varies, and may cause the algorithm to classify ‘slow walking’ for some subjects as ‘normal walking’ for others. The same reason would explain the misclassifications between ‘G5’ and ‘G7’, as those gaits are carefully chosen to be similar in pairs for creating more classification challenges. For the last two joint gaits which contain a fall event, the correctly classified rate is not too low. However, there are some false alarms with other classes, and this affects a lot the capability of recognizing critical events like falls.

TABLE III. THE L1O CLASSIFICATION RESULTS FOR SINGLE RADAR SENSORS (MAX, MIN, MEAN AND STANDARD DEVIATION)

Linear SVM	Ancortek	X1	X2	X3
<i>Mean</i>	58.53%	<b>59.13%</b>	58.33%	49.6%
<i>Max</i>	80.56%	80.56%	72.22%	66.67%
<i>Min</i>	36.11%	19.44%	38.89%	25%
<i>STD</i>	0.1393	0.165	<b>0.101</b>	0.1293
RF Bagging	Ancortek	X1	X2	X3
<i>Mean</i>	59.52%	59.72%	<b>63.49%</b>	54.17%
<i>Max</i>	75%	77.78%	83.33%	77.78%
<i>Min</i>	38.89%	36.11%	44.44%	33.33%
<i>STD</i>	0.1246	0.1241	0.1251	0.1172

### B. Transfer Learning using Pre-trained Networks

Transfer learning [19], [20] has attracted a lot of interest in the field of image classification in applications such as face and gesture recognition. Fig. 4 illustrates the training and testing scheme of the transfer learning with a VGG-16 net taken as an example. It uses the output weights from a deep neural network pre-trained on numerous optical images, which enables the network to capture the common concepts among the edges, curves, and other properties of the figure patterns. This can lead to a potential application that makes this network capable of adapting to a new dataset by re-training with a small amount of the new labeled data, radar data in this case, and fine-tuning the original weights.

Transfer learning uses a pre-trained network, and this solves specific issues of the classic Convolution Neural Networks (CNN). Notably, it does not require a large dataset to train, and as a result of that, it saves a lot of training time and computational load. In this paper, five pre-trained networks, notably AlexNet, GoogLeNet, VGG-16, ResNet18, and ResNet101, are empirically selected to re-train with radar spectrograms and compare the classification performance.

Table IV lists the classification performance of each radar using a pre-trained net in terms of mean, maximum, minimum,



and standard deviation across the leave one participant out (L1O) tests for the 14 subjects. From the perspective of average performance, VGG-16 outperforms the other pre-trained networks, where the Xethru radar on the ceiling yields the best results among all the available radars. It is reported that Ancortek radar using ResNet101 provides better average performance than VGG-16, which seems to show that ResNet101 is more powerful in characterizing the features from Ancortek images.

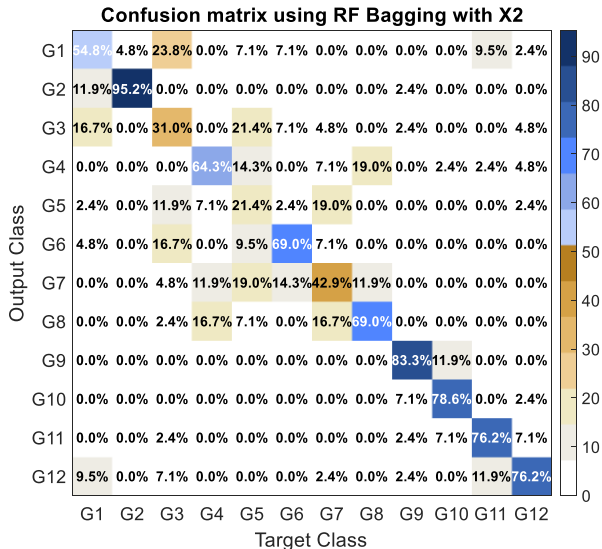


Fig. 3. Confusion matrix of Xethru P2 using RF Bagging Trees

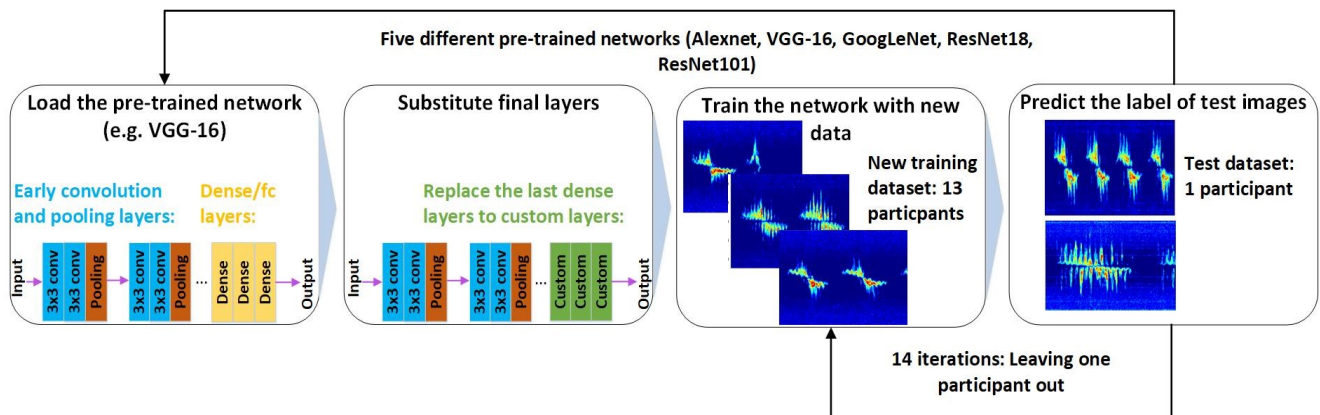


Fig. 4. The training and testing scheme of transfer learning.

#### IV. INFORMATION FUSION

In the circumstance that the participant is moving in a large angle with respect to the radar line-of-sight, the receiving signal strength is not optimal due to the well-known aspect angle problem. This may lead to possible misclassification and false alarms. However, the low classification performance of one radar at a certain time could be mitigated by using the data of other radars working at different frequency bands and placed at different locations in a radar network.

The fusion of radar data can take place at feature and decision level separately. Feature fusion physically cascades the feature subset from each radar to a feature pool, as in Eq. 1, where  $\smile$  represents the concatenation of the feature matrices of individual radar sensors.

$$F_{Fusion} = F_{An} \smile F_{X_1} \smile F_{X_2} \smile F_{X_3} \quad (1)$$

TABLE IV. THE L1O CLASSIFICATION RESULTS USING PRE-TRAINED NETWORKS ON DATA FROM SINGLE RADAR SENSORS

Alexnet	Ancortek	X1	X2	X3
<i>Mean</i>	67.86%	71.83%	71.83%	64.88%
<i>Max</i>	83.33%	86.11%	91.67%	86.11%
<i>Min</i>	50%	47.22%	44.44%	38.89%
<i>STD</i>	0.1179	0.1308	0.1517	0.1483
VGG-16	Ancortek	X1	X2	X3
<i>Mean</i>	73.41%	75.2%	79.96%	71.23%
<i>Max</i>	91.67%	91.67%	94.44%	83.33%
<i>Min</i>	47.22%	47.22%	63.89%	50%
<i>STD</i>	0.1202	0.1372	0.1069	0.1236
GoogLeNet	Ancortek	X1	X2	X3
<i>Mean</i>	66.47%	60.52%	62.9%	55.95%
<i>Max</i>	80.56%	83.33%	80.56%	75%
<i>Min</i>	47.22%	44.44%	47.22%	38.89%
<i>STD</i>	0.1114	0.1199	0.1048	0.1050
ResNet18	Ancortek	X1	X2	X3
<i>Mean</i>	71.83%	63.89%	66.27%	60.52%
<i>Max</i>	86.11%	80.56%	80.56%	72.22%
<i>Min</i>	58.33%	52.78%	55.56%	47.22%
<i>STD</i>	0.0936	0.0844	0.0864	0.0845
ResNet101	Ancortek	X1	X2	X3
<i>Mean</i>	76.19%	68.85%	66.87%	60.32%
<i>Max</i>	88.89%	83.33%	77.78%	77.78%
<i>Min</i>	55.56%	52.78%	52.78%	33.33%
<i>STD</i>	0.1009	0.0831	0.0640	0.1244

Decision fusion is divided into soft fusion and hard fusion. Soft fusion uses the confidence level of the separate classifiers to generate the new prediction label. If a weighted index is introduced for each radar, then the approach becomes weighted soft fusion as in Eq. 2.

$$S_{fusion}(n, c) = W_{An} \cdot S_{An}(n, c) + W_{X_1} \cdot S_{X_1}(n, c) + W_{X_2} \cdot S_{X_2}(n, c) + W_{X_3} \cdot S_{X_3}(n, c) \quad (2)$$

In Eq. 2,  $S(n, c)$  refers to the confidence level for observation  $n$  and class  $c$ ,  $W_{An}$  to  $W_{X_3}$  denote the weight coefficients for each radar, respectively. Generally, the radar with high individual classification performance is associated to higher weights. Hard fusion relies on the posterior probability of the class of interest in the confusion matrix to make a new decision. Typical hard fusion methods include majority voting, weighted majority voting, recall combiner, and Naive-Bayes (NB) combiner [24]. Voting system usually suffers

from decision clash when the number of classifiers is even in the fusion. The performance of the recall combiner is highly correlated with number of classifiers, as small number of classifiers such as our case cannot fully exploit the potential of recall combiner. However, the influence of classifier numbers is much less on NB combiner approach.

$$P(C_k|d) = P(C_k) \cdot \prod_{m=1}^N p_{m,R_m,k} \quad (3)$$

Eq. (3) shows the mathematical representation of an NB combiner, where  $k$  is the class of interest and  $d$  is a class set including all the classes to classify.  $P(C_k|d)$  is the probability that class  $k$  is chosen from the class set  $d$  to be the output class and  $P(C_k)$  is the classifier support rate.  $R_m$  denotes the prediction label of classifier  $m$ , whereas the output is the product of the support rate and the element  $p$  of the radar confusion matrix (classifier  $m$ , row  $R_m$  and column  $k$ ). From the results in our previous work [21], NB combiner is chosen as the main information fusion approach. Feature level fusion and equal weighted soft fusion are also considered as alternatives for comparison with conventional classifier and transfer learning respectively.

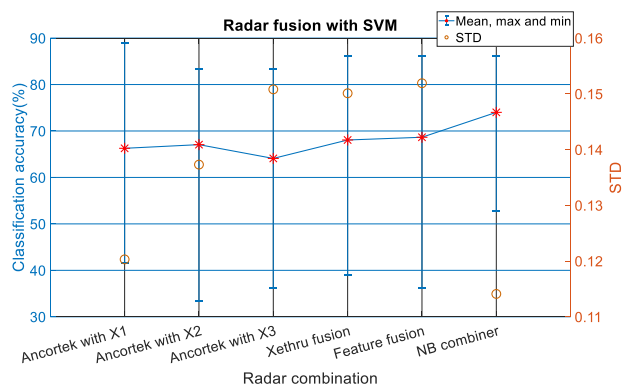


Fig. 5. The statistical parameters (classification accuracy in percentage and standard deviation of the values) for individual radar sensors and different fusion techniques using classifier SVM.

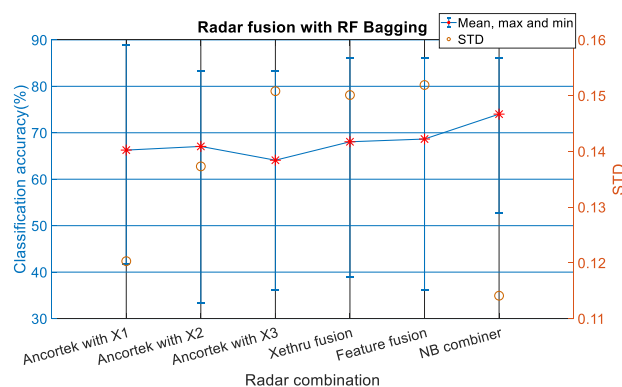


Fig. 6. The statistical parameters (classification accuracy in percentage and standard deviation of the values) for individual radar sensors and different fusion techniques using classifier RF Bagging.

Fig. 5-6 illustrate the statistical parameters for the radar fusion (average accuracy and standard deviation of the classification accuracy) with SVM and RF Bagging Trees. Different combinations of different radars are considered. Note that in the figures, “feature fusion” and “NB combiner” cases included data from all the radar sensors in the network. For the SVM, fusion with all radars with NB combiner yields the best classification performance, approximately 4% and 19% higher than the best and worst case in the single radar

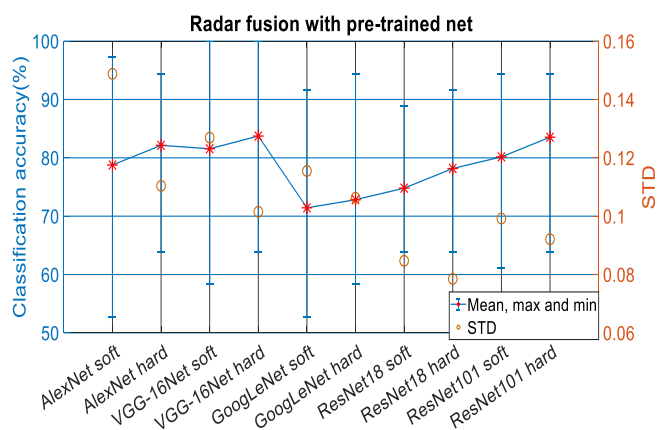


Fig. 7. The statistical parameters (classification accuracy in percentage and standard deviation of the values) of soft and hard fusion with all the radars in the network using transfer learning with different networks

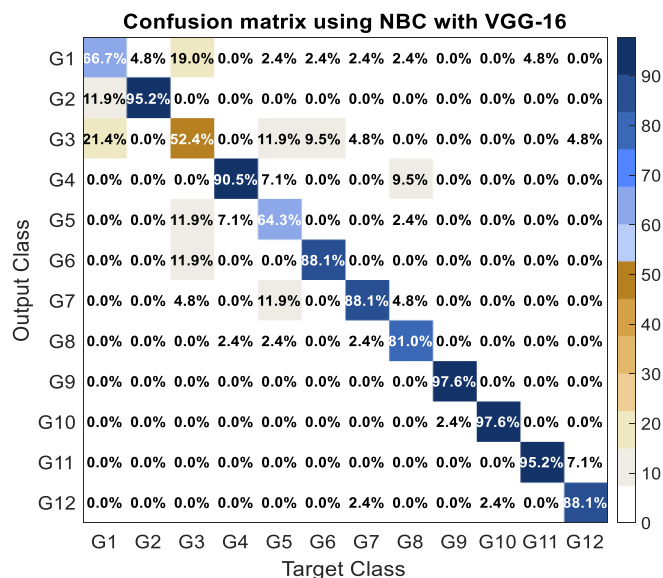


Fig. 8. Confusion matrix of Naïve Bayes combiner hard fusion with VGG-16 network.

scenario. Additionally, significant improvement (about 6% and 7%) is reported by combining the Ancortek radar with X1 and X2 at the feature level.

Fig. 7 shows the same performance parameters for fusion of all radar sensors using pre-trained networks. VGG-16 surpasses the other networks in both hard and soft fusion, whereas ResNet101 is only 0.5% lower in hard fusion. The main benefit of transfer learning is increasing the minimum accuracy (i.e. worst case performance) to 64%, which is 12% higher than the same approach with RF Bagging Trees. At the same time, the standard deviations of transfer learning are lower than for conventional classifiers; in other words, the variation of performance based on the participants used as testing subjects is lower, and this leads to a more stable system.

Fig. 8 discusses the misclassification between classes using NB combiner hard fusion with a VGG-16 pre-trained network. Compared to Fig. 3, the classification accuracy rises to 83.73%, and most of the misclassified events are corrected, whereas the wrong classified gaits between ‘G1’ and ‘G3’ are still existing but less than before. The classification rates of ‘G5’ and ‘G7’ are improved significantly by 43% and 46%, respectively. Additionally, the false alarms of falling in ‘G11’ and ‘G12’ are much lower than using X2 individually.

## V. CONCLUSION

This paper presents an information fusion framework applied on radar data from a network of four coordinated sensors, namely three UWB Xethru radar and one FMCW Ancortek radar. Conventional classifiers and transfer learning approaches with five different pre-trained deep networks are compared, with the aim of recognizing different gait styles and identifying fall accidents.

The data from four different radar systems are combined at feature and decision level to provide subsequent improvement of 4-20% compared with the best case of using radar individually. It is reported that Naïve Bayes combiner (NBC) based on the posterior probability of the class of interest outperforms other fusion techniques. In terms of the classifier, VGG-16 yields the best classification performance among SVM, RF Bagging Trees, and other pre-trained networks. Data fusion using NBC with VGG-16 indicates approximately 84% average classification accuracy after considering all the participants as test subjects.

Future work will evaluate the information fusion method on a wider platform. This includes more participants, more aspect angles with the radar, and even multimodal approaches as seen in [25]. Regarding the neural network, a sequential classification task, as seen in [21] with continuous gaits and motion transitions will be considered, as well as the meta-learning of the hyper-parameters and structure of the pre-trained network.

## ACKNOWLEDGMENT

The authors are grateful to the colleagues in the CI4R lab for their participation and help in the data collection.

## REFERENCES

- [1] W. H. O. Ageing and L. C. Unit, "WHO global report on falls prevention in older age," *World Heal. Organ.*, 2008.
- [2] K. Chaccour, R. Darazi, A. H. El Hassani, and E. Andr s, "From fall detection to fall prevention: A generic classification of fall-related systems," *IEEE Sens. J.*, vol. 17, no. 3, pp. 812–822, 2017.
- [3] C. S. Florence, G. Bergen, A. Atherly, E. Burns, J. Stevens, and C. Drake, "Medical costs of fatal and nonfatal falls in older adults," *J. Am. Geriatr. Soc.*, 2018.
- [4] M. Mubashir, L. Shao, and L. Seed, "A survey on fall detection: Principles and approaches," *Neurocomputing*, vol. 100, pp. 144–152, 2013.
- [5] NIHR Dissemination Centre, "HELP AT HOME Use of assistive technology for older people," *Natl. Inst. Heal. Res.*, pp. 3–6, 2018.
- [6] F. Wang, M. Skubic, M. Rantz, and P. E. Cuddihy, "Quantitative Gait Measurement With Pulse-Doppler Radar for Passive In-Home Gait Assessment," *IEEE Trans. Biomed. Eng.*, vol. 61, no. 9, pp. 2434–2443, 2014.
- [7] H. Wang, D. Zhang, Y. Wang, J. Ma, Y. Wang, and S. Li, "RT-Fall: A real-time and contactless fall detection system with commodity WiFi devices," *IEEE Trans. Mob. Comput.*, vol. 16, no. 2, pp. 511–526, 2017.
- [8] X. Bai, Y. Hui, L. Wang, and F. Zhou, "Radar-Based Human Gait Recognition Using Dual-Channel Deep Convolutional Neural Network," *IEEE Trans. Geosci. Remote Sens.*, vol. 57, no. 12, pp. 9767–9778, 2019.
- [9] A. Seifert, M. G. Amin, and A. M. Zoubir, "Toward Unobtrusive In-Home Gait Analysis Based on Radar Micro-Doppler Signatures," *IEEE Trans. Biomed. Eng.*, vol. 66, no. 9, pp. 2629–2640, 2019.
- [10] A. Seifert, A. M. Zoubir, and M. G. Amin, "Detection of Gait Asymmetry Using Indoor Doppler Radar," in *2019 IEEE Radar Conference (RadarConf)*, 2019, pp. 1–6.
- [11] H. Li *et al.*, "Multisensory Data Fusion for Human Activities Classification and Fall Detection," in *2017 IEEE Sensors Conference*, 2017, pp. 1-3.
- [12] H. Li, A. Shrestha, H. Heidari, J. L. Kerne , and F. Fioranelli, "Magnetic and Radar Sensing for Multimodal Remote Health Monitoring," *IEEE Sens. J.*, vol. 19, no. 20, pp. 8979–8989, 2018.
- [13] T. R. Bennett, J. Wu, N. Kehtarnavaz, and R. Jafari, "Inertial measurement unit-based wearable computers for assisted living applications: A signal processing perspective," *IEEE Signal Process. Mag.*, vol. 33, no. 2, pp. 28–35, 2016.
- [14] D. Wu *et al.*, "Deep Dynamic Neural Networks for Multimodal Gesture Segmentation and Recognition," *IEEE Trans. Pattern Anal. Mach. Intell.*, vol. 38, no. 8, pp. 1583–1597, 2016.
- [15] P.-H. Chen, M. C. Shastry, C.-P. Lai, and R. M. Narayanan, "A portable real-time digital noise radar system for through-the-wall imaging," *IEEE Trans. Geosci. Remote Sens.*, vol. 50, no. 10, pp. 4123–4134, 2012.
- [16] B. Erol and M. G. Amin, "Radar Data Cube Processing for Human Activity Recognition Using Multi Subspace Learning," *IEEE Trans. Aerosp. Electron. Syst.*, 2019.
- [17] Y. Kim and T. Moon, "Human detection and activity classification based on micro-Doppler signatures using deep convolutional neural networks," *IEEE Geosci. Remote Sens. Lett.*, vol. 13, no. 1, pp. 8–12, 2016.
- [18] J. Le Kerne  *et al.*, "Radar Signal Processing for Sensing in Assisted Living: The challenges associated with real-time implementation of emerging algorithms," *IEEE Signal Process. Mag.*, vol. 36, no. 4, pp. 29–41, 2019.
- [19] A. Shrestha *et al.*, "Cross-Frequency Classification of Indoor Activities with DNN Transfer Learning," in *2019 IEEE Radar Conference (RadarConf)*, 2019, pp. 1–6.
- [20] S. Z. Gurbuz and M. G. Amin, "Radar-Based Human-Motion Recognition With Deep Learning: Promising applications for indoor monitoring," *IEEE Signal Process. Mag.*, vol. 36, no. 4, pp. 16–28, 2019.
- [21] H. Li, A. Shrestha, H. Heidari, J. Le Kerne , and F. Fioranelli, "Bi-LSTM Network for Multimodal Continuous Human Activity Recognition and Fall Detection," *IEEE Sens. J.*, vol. 20, no. 3, pp. 1191–1201, 2020.
- [22] S. Z. Gurbuz, B. Erol, B.  a hyan, and B. Tekeli, "Operational assessment and adaptive selection of micro-Doppler features," *IET Radar, Sonar Navig.*, vol. 9, no. 9, pp. 1196–1204, 2015.
- [23] F. Fioranelli, M. Ritchie, S. Z. Gurbuz, and H. Griffiths, "Feature diversity for optimized human micro-Doppler classification using multistatic radar," *IEEE Trans. Aerosp. Electron. Syst.*, vol. 53, no. 2, pp. 640–654, 2017.
- [24] L. Kuncheva and J. Rodr guez, "A weighted voting framework for classifiers ensembles," *Knowledge and Information Systems*, vol. 38, 2014.
- [25] E. Cippitelli, F. Fioranelli, E. Gambi, and S. Spinsante, "Radar and RGB-depth sensors for fall detection: a review," *IEEE Sens. J.*, vol. 17, no. 12, pp. 3585–3604, 2017.